



Cite this: DOI: 10.1039/d6gc00784h

## Establishing parameters for resonant acoustic mixing (RAM) chemistry using Buchwald–Hartwig amination as a model

Lori Gonnet, <sup>a</sup> Cameron B. Lennox, <sup>a,b</sup> Tristan H. Borchers,<sup>a</sup> Mohammad S. Askari, <sup>a</sup> Alexander Wahrhaftig-Lewis,<sup>a</sup> Stefan G. Koenig, \*<sup>c</sup> Karthik Nagapudi \*<sup>c</sup> and Tomislav Friščić \*<sup>a</sup>

While Resonant Acoustic Mixing (RAM) has been proposed as a scalable methodology for environmentally-friendly synthesis, notably media-free mechanochemical synthesis, the underlying reaction environment and the parameters that govern reaction control, optimization, and scale-up remain poorly understood. Using the Buchwald–Hartwig amination as a model system, this study provides insight into the RAM reaction environment and establishes design parameters through a combination of systematic screening and multi-modal, real-time *in situ* monitoring of reaction progress, temperature evolution, and the transformations of crystalline and non-crystalline bulk phases. The simultaneous application of benchtop infrared thermography, and fingerprint- and terahertz-region Raman (THz-Raman) spectroscopy enables the direct correlation of reactivity, thermal behaviour, and phase evolution. Specifically, this work identifies the filling ratio ( $\varphi$ ), acceleration, and the amount of liquid additive ( $\eta$ ) as critical parameters to design tunable and scalable (at least 100 mmol) reactivity under RAM conditions, in short timeframes. Real-time monitoring reveals that rapid Buchwald–Hartwig reactivity is associated with autogenous heating, and that  $\varphi$  and acceleration serve as parameters that can be used to control reaction kinetics and temperature evolution. By identifying experimentally accessible reaction control parameters and presenting a benchtop-only design for the simultaneous monitoring of temperature, reaction progress and evolution of transient bulk phases, this work provides a foundation for the rational design, control, and safety of chemistry under RAM conditions.

Received 5th February 2026,  
Accepted 18th February 2026

DOI: 10.1039/d6gc00784h

rsc.li/greenchem

### Green foundation

1. This work advances green chemistry by establishing key parameters to design and control reactions using Resonant Acoustic Mixing (RAM) – an emergent, scalable alternative to conventional milling mechanochemistry.
2. This work establishes reactor filling ratio as an important parameter to design RAM-based reactions without bulk solvents, and presents a benchtop methodology for simultaneous real-time following of reaction kinetics, structure of bulk phases, and temperature. Using Buchwald–Hartwig amination as a model, the value of real-time monitoring is evidenced by revealing short-lived temperature increases, means of controlling them, and their role for achieving rapid, high-yielding, multi-gram transformations.
3. This work is a stepping stone towards the rational design of green, RAM-based reactions and could further be enhanced by a deeper understanding of thermal behaviour and how it could be effectively controlled for scale-up, reducing catalyst amount, and promoting reactivity of more challenging substrates.

## Introduction

Resonant Acoustic Mixing (RAM)<sup>1</sup> is a highly efficient mixing technology that has recently been used as a scalable technique

for chemical<sup>2–6</sup> and material<sup>7–12</sup> synthesis, as well as for high-throughput reaction and cocrystal screening.<sup>13–15</sup> The efficiency and speed of mixing of materials with different rheology has introduced RAM as a highly effective approach for making blends, composites, and materials processing.<sup>16–19</sup> Recently, RAM has also been used to conduct chemical transformations in the absence of bulk solvent, under solventless or liquid-assisted conditions otherwise accessible with mechanochemical technologies such as grinding or ball-milling.<sup>10–15</sup> By delivering mechanical energy through high-intensity, low-frequency acoustic oscillation of the entire system, RAM is seen as a “ball-free” alternative to conventional mechanochemical

<sup>a</sup>School of Chemistry, University of Birmingham, Edgbaston, Birmingham, B15 2TT, UK. E-mail: t.frisic@bham.ac.uk

<sup>b</sup>Department of Chemistry, McGill University, 801 Sherbrooke St. W., H3A 0B8 Montreal, Canada

<sup>c</sup>Synthetic Molecule Pharmaceutical Sciences, Genentech Inc., One DNA Way, South San Francisco, CA 94080, USA. E-mail: koenig.stefan@gene.com, nagapudi.karthik@gene.com



technologies<sup>20</sup> that rely on continuously moving balls, rods, or screws to impart mechanical energy.<sup>21–23</sup> By eliminating these mechanical elements, also known as milling media, RAM significantly simplifies reaction design, facilitates scale-up, and is expected to minimise or even avoid contamination arising as a result of abrasion from the grinding media. Whereas the potential for high-throughput screening, as well as simplicity of reaction scale-up have been demonstrated in the contexts of material chemistry and catalysis, the parameters which can be used to control and optimize RAM-based reactivity remain poorly understood.

Using as a model the palladium-catalysed Buchwald–Hartwig amination (Fig. 1), arguably one of the key transformations in pharmaceutical and medicinal chemistry<sup>24,25</sup> which is also known to provide safety-related challenges,<sup>26</sup> we now provide a detailed investigation of parameters that can be used to control and optimize RAM-based reactions. This is achieved through extensive screening, real-time *in situ* infrared temperature monitoring (thermography),<sup>27,28</sup> as well as fingerprint Raman, and low-frequency (terahertz, THz) Raman spectroscopy, which enabled an entirely benchtop-based approach to simultaneously gain insight into temperature evolution, reaction kinetics and transformations of bulk crystalline and non-crystalline phases, which would normally require the use of synchrotron X-ray diffraction.<sup>28</sup> Whereas recent work has demonstrated the ability to optimize RAM reactivity through the presence and the amount of liquid additives, as well as by

varying the acceleration of the reaction vessels (expressed in the acceleration of gravity,  $g = 9.81 \text{ m s}^{-2}$ ),<sup>4–9</sup> it is now shown that the degree of reactor loading, expressed as the filling ratio ( $\varphi$ , the ratio of the reaction mixture volume to the volume of the reaction vessel), can play a critical role in controlling reactivity under RAM conditions. Notably, while recent reports explored how the filling ratio can affect the blending efficiency in RAM, the relationship of  $\varphi$  to chemical reactivity under RAM conditions remains poorly explored.<sup>29,30</sup> Here, the Buchwald–Hartwig amination was chosen as a suitable model for such studies, as it was previously investigated using mechanochemical ball-milling,<sup>31–35</sup> thermochemical,<sup>36–39</sup> or combined thermo-mechanical<sup>40</sup> approaches. We show how varying  $\varphi$ , acceleration, and addition of a liquid additive (expressed as  $\eta$ ,<sup>41,42</sup> the ratio of the volume of the liquid additive to the total mass of the reaction mixture, in  $\mu\text{L mg}^{-1}$ ) can be used to affect reaction kinetics and associated thermal behaviour, which is of importance in context of reaction design and safety (Fig. 1). Whereas Buchwald–Hartwig coupling under solventless and ball-milling conditions was previously promoted by external heating,<sup>43</sup> our results show that in RAM such reactivity can be promoted by autogenous heating, without an external heat source, when operating at high values of  $\varphi$  and acceleration. This leads to rapid (typically within 10–15 minutes), high-yielding, multigram-scale transformations of solid and liquid reactants, with a model reaction scaled to 100 mmol, as well as ability to obtain triaryl amines, in high conversion compared to corresponding diarylamines, starting from simple aniline precursors. Together with more conventionally used parameters, such as reaction time and catalyst amount, the herein explored variables  $\varphi$ ,  $\eta$ , and acceleration provide a broad, versatile set of reaction control parameters under RAM conditions.

## Results and discussion

As a benchmark reaction, we focused on the Buchwald–Hartwig coupling of two solid reactants, 1-bromopyrene and diphenylamine, to give **1a** (Fig. 2a), which was previously also explored by ball-milling.<sup>33</sup> We conducted the RAM reactions using the LabRAM II instrument, typically in commercial 2.5 mL volume polypropylene vials. An equimolar mixture of reactants (0.25 mmol) in the presence of 3 mol% first-generation (G1) XPhos-Pd catalyst<sup>37</sup> and two equivalents of sodium *tert*-butoxide (NaOtBu) base was subjected to RAM at 60g for 60 minutes. Analysis of the crude reaction mixture by <sup>1</sup>H NMR after dissolution in CDCl<sub>3</sub> revealed no product formation, consistent with the previously reported lack of reactivity upon neat milling.<sup>33</sup> Next, we explored the effect of adding a small amount of liquid additive, in the  $\eta$ -range from 0 to 1.5  $\mu\text{L mg}^{-1}$ . These conditions are consistent with those typically used in liquid-assisted mechanochemistry.<sup>42,44</sup> After 60 minutes of RAM at 60g in the presence of tetrahydrofuran (THF), <sup>1</sup>H NMR analysis of the crude reaction mixture revealed

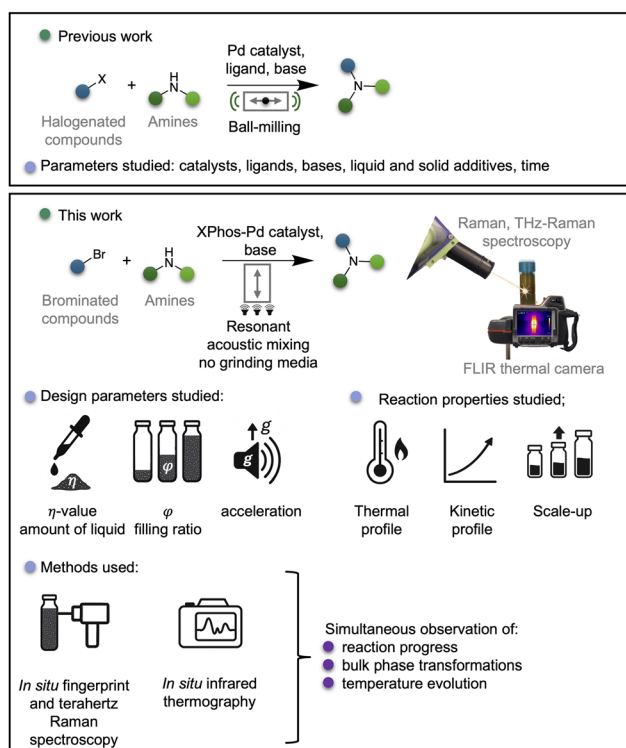


**Fig. 1** Comparison of the methods and parameters addressed in previous studies<sup>31–35</sup> of mechanochemical Buchwald–Hartwig reactivity by ball-milling, and in the present investigation of RAM-based reactivity.



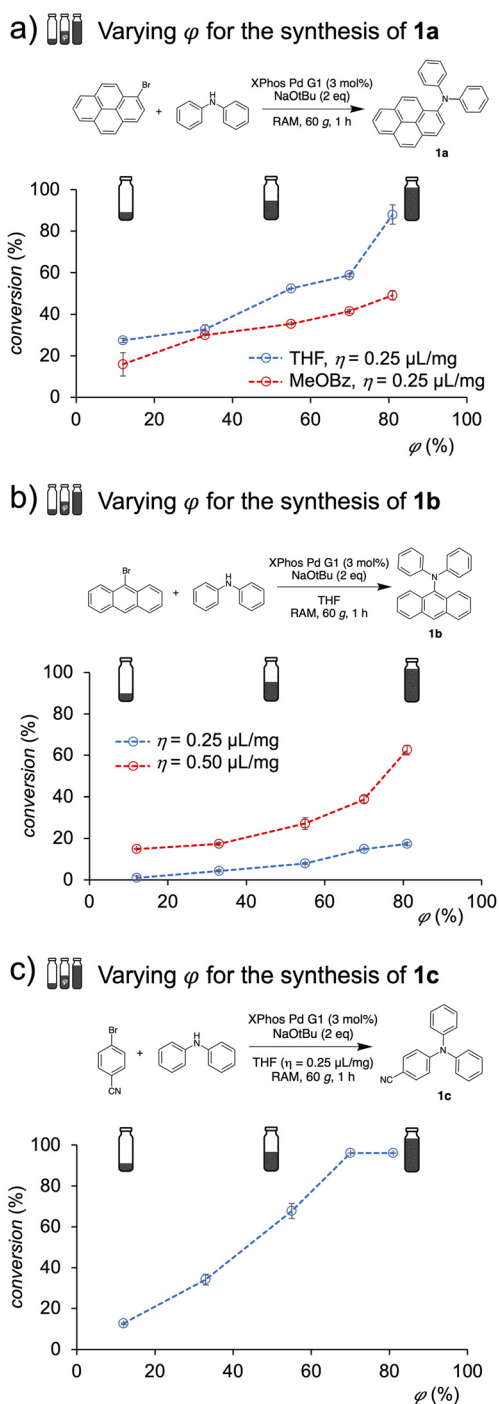


**Fig. 2** Dependence of the Buchwald–Hartwig amination reactivity in RAM on the filling ratio ( $\phi$ ) for the coupling of (a) 1-bromopyrene (solid) and diphenylamine (solid) to form **1a** in presence of THF or MeOBz ( $\eta = 0.25 \mu\text{L mg}^{-1}$ ) as the liquid additive; (b) diphenylamine and 9-bromoanthracene (solid) to form **1b** in presence of THF at different  $\eta$ -values ( $\eta = 0.25$  and  $0.50 \mu\text{L mg}^{-1}$ ); (c) diphenylamine (solid) with 4-bromobenzonitrile (solid) to give product **1c** in presence of THF ( $\eta = 0.25 \mu\text{L mg}^{-1}$ ). Corresponding plots with respect to reaction scale are shown in SI Fig. S4. All  $\phi$  values are approximate and correspond to the filling level of the initial reaction mixture, before the onset of RAM.

a monotonic increase in conversion to **1a** with increasing  $\eta$ , reaching a plateau at *ca.* 50% conversion (SI Fig. S3).

However, increasing the reaction scale, without altering the size of the reaction vessel, led to a significant improvement in reactivity. The conversion was found to generally increase with respect to  $\phi$  (Fig. 2a),<sup>3,45</sup> which was estimated by comparing the height of the reaction mixture in the vial before the RAM experiment to the height of the vial. The filling ratio estimated in this way should be taken as an approximation, as the reaction mixture volume is likely to change upon intense mixing and during reaction. While the initial experiments were performed at *ca.*  $\phi = 10$ –15%, increasing the filling ratio led to improved conversions, reaching *ca.* 90% at a  $\phi$ -value of *ca.* 80%, based on <sup>1</sup>H NMR analysis after 60 minutes of RAM. To ensure that the analysis is not affected by sample preparation time, selected reactions were analysed by either first quenching the residual strong base using water, followed by extraction into CDCl<sub>3</sub>, or by directly dissolving the reaction mixture in CDCl<sub>3</sub>. Both methods of analysis gave comparable results (SI Fig. S5). Overall, the aforementioned observations suggest  $\phi$  as a previously not reported parameter to optimize reactions in RAM. It is worth noting that reactions by ball-milling generally perform worse with increased filling ratio<sup>3,45</sup> as the additional material hinders the motion of milling media, reducing mixing and energy transfer. The improvement in reactivity by increasing the reactor volume occupied by reactants, therefore highlights a fundamental difference in reaction design between RAM and ball-milling.

To test the generality of using  $\phi$  to modify reaction conversion, the coupling of diphenylamine was further explored with 9-bromoanthracene and 4-bromobenzonitrile, to give **1b** and **1c**, respectively (Fig. 2b and c). These reactions similarly showed a notable improvement in conversion with increasing  $\phi$ . Similar behaviour was also seen when using a different liquid additive, methyl benzoate (MeOBz) (Fig. 2a), as well as when using different combinations of liquid and solid reactants such as *N*-methylaniline (liquid) with bromobenzene (liquid) or with 4-bromobenzonitrile (solid), respectively (SI Fig. S6). The latter transformation was also attempted using alternative bases, such as KO<sup>t</sup>Bu, LiO<sup>t</sup>Bu and NaOMe, but gave poorer results (SI Table S11). The use of MeOBz as the liquid additive (Fig. 2a) was of particular interest as a more environmentally-friendly, high-boiling alternative (boiling point 200 °C) to THF (boiling point 66 °C), suitable for exothermic or elevated temperature reactions. While conversion for each of the explored reactions improved with  $\phi$ , the dependence of conversion on filling ratio was in each case different, possibly reflecting the complexity of the still unclear relationship between filling ratio and mixing.<sup>29,30</sup> Overall, these results present  $\phi$  as a parameter to design and control reactions under resonant acoustic mixing conditions.

Next, we explored how changes to acceleration affect reactivity, by conducting the synthesis of **1a** at 80g and 100g, resulting in <sup>1</sup>H NMR conversions of >95% after *ca.* 15 and 10 minutes, respectively. This is a notable reduction in reaction time compared to 60 minutes previously reported for ball-milling in the



presence of 5 mol% Pd(OAc)<sub>2</sub>, tris(*tert*-butyl)phosphine and NaOtBu.<sup>33</sup> The rapid reaction under RAM conditions led us to consider the potential importance of frictional heating on reactivity and, for this purpose, the opaque 2.5 mL volume polypropylene vessels were replaced with optically transparent commercial 5 mL volume borosilicate glass vials suitable for infrared temperature monitoring (thermography) using a forward-looking infrared (FLIR) camera (SI Fig. S1 and S2). Whereas no incidents were encountered in this work, it should be kept in mind that using glass vials could represent a hazard. To verify that the reactions conducted in 5 mL glass vials are consistent with those obtained in 2.5 mL polypropylene vials, selected reactions were conducted in both reactor types at approximately the same  $\varphi$ , showing overall similar results (SI Table S12). Real-time evolution of the reaction temperature was initially monitored for the RAM synthesis of **1a** at 100g and  $\varphi = 80\%$  (Fig. 3 and SI Fig. S10), over 60 minutes.

In the absence of the palladium catalyst, no reaction is observed, and thermographic monitoring showed a monotonic increase in temperature from *ca.* 20 °C to 50 °C over *ca.* 20 minutes, after which the temperature remained relatively constant. This measurement, conducted in duplicate, provides an estimate of frictional heating upon RAM at 100g in the absence of Buchwald amination reaction. A very different temperature profile was observed, however, in the presence of 3 mol% palladium catalyst, revealing a short-lived (*ca.* 5–10 minutes) increase and decrease in temperature soon after initiating mixing, reaching a maximum of *ca.* 85 °C, and then rapidly falling to *ca.* 30 °C. We attribute the higher final temperature of the non-reactive system in the absence of a catalyst,

compared to the reaction mixture in the presence of the catalyst, to both chemical, as well as rheological differences. On one hand, the system without the catalyst remained a thick paste that allowed for sustained frictional heating, while the reaction mixture in the presence of the catalyst underwent a change in chemical composition and became more solid, reducing the capacity for frictional heating. On the other hand, it is also likely that difference in heat capacities of the two reaction mixtures, resulting from a change in chemical composition once the reaction has taken place, plays a role.

The appearance of exotherms during Buchwald–Hartwig reaction has been previously reported, and represents an important consideration for reaction scalability and safety.<sup>26</sup> To further investigate the relationship between the appearance of the thermal spike and reaction conversion, the reaction was tracked in real time at accelerations of 60g, 80g and 100g using simultaneous thermographic monitoring and Raman spectroscopy in both the fingerprint (200–1400 cm<sup>-1</sup>) and low-frequency (THz, from the Rayleigh line to 200 cm<sup>-1</sup>)<sup>46</sup> regions. Whereas fingerprint Raman spectroscopy permits direct insight into reaction kinetics, monitoring in the THz-region was recently shown to also permit detecting the appearance and disappearance of bulk crystalline phases,<sup>47</sup> providing a route for simultaneous tracking of changes in molecular, as well as extended crystal structure of substances.<sup>47,48</sup> The ability to track the crystallinity of reaction components by benchtop THz-Raman spectroscopy, rather than by currently ubiquitous synchrotron X-ray diffraction, presents an exciting opportunity to gain insight into the phase behaviour of mechanochemical and/or solventless reactions, which has generally been limited to qualitative visual observations or calorimetric experiments.<sup>49–52</sup> To ensure reproducibility, each monitoring experiment was performed in triplicate (see SI Fig. S10–12).

For reactions at 100g, the temperature profile consistently revealed a sharp, short-lived temperature increase to *ca.* 80 °C within the first 6 minutes of RAM (Fig. 3, 4 and SI Fig. S10). A similar, but lower, spike in temperature (up to ~75 °C) was observed within 10 minutes for the reactions conducted at 80g (Fig. 4 and SI Fig. S11). At 60g, however, the temperature maximum was much less pronounced, reaching no more than *ca.* 34 °C (Fig. 4 and SI Fig. S12). Raman spectroscopy enabled following the progress of the reaction in real time, by tracking the disappearance of reactant bands at 574 cm<sup>-1</sup> and 621 cm<sup>-1</sup> assigned to 1-bromopyrene, and the appearance of **1a** product bands at 611 cm<sup>-1</sup> and 1395 cm<sup>-1</sup>. Tracking the **1a** band at 611 cm<sup>-1</sup> revealed that the reactions at 80g and 100g exhibit sigmoidal behaviour: in both cases, the formation of **1a** is initially slow with up to *ca.* 10% conversion, but then advances rapidly around 5 minutes (for 100g) or 8 minutes (for 80g) of RAM. The rapid increase in conversion coincided well with the spike in reaction temperature (Fig. 4, SI Fig. S10 and S11), consistent with Buchwald–Hartwig coupling reactions being accelerated at elevated temperatures.<sup>40,45</sup> Subsequent analysis of the reaction mixtures by <sup>1</sup>H NMR indicated that at 100g and 80g the reactions are effectively complete after 10 and 15 minutes of RAM with *ca.* 96% and 92% reactant conversion,

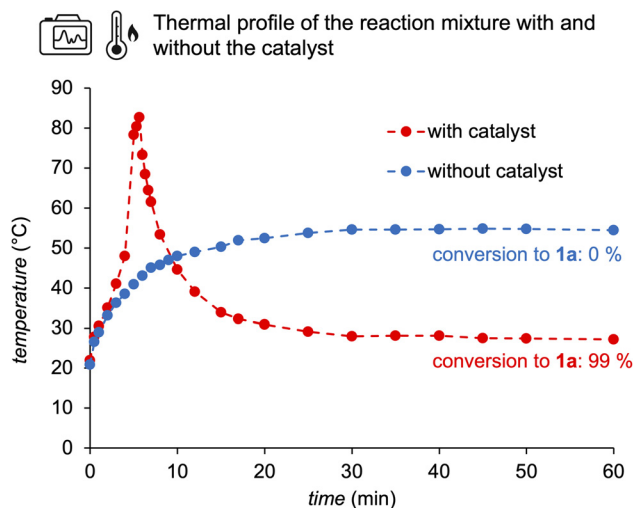
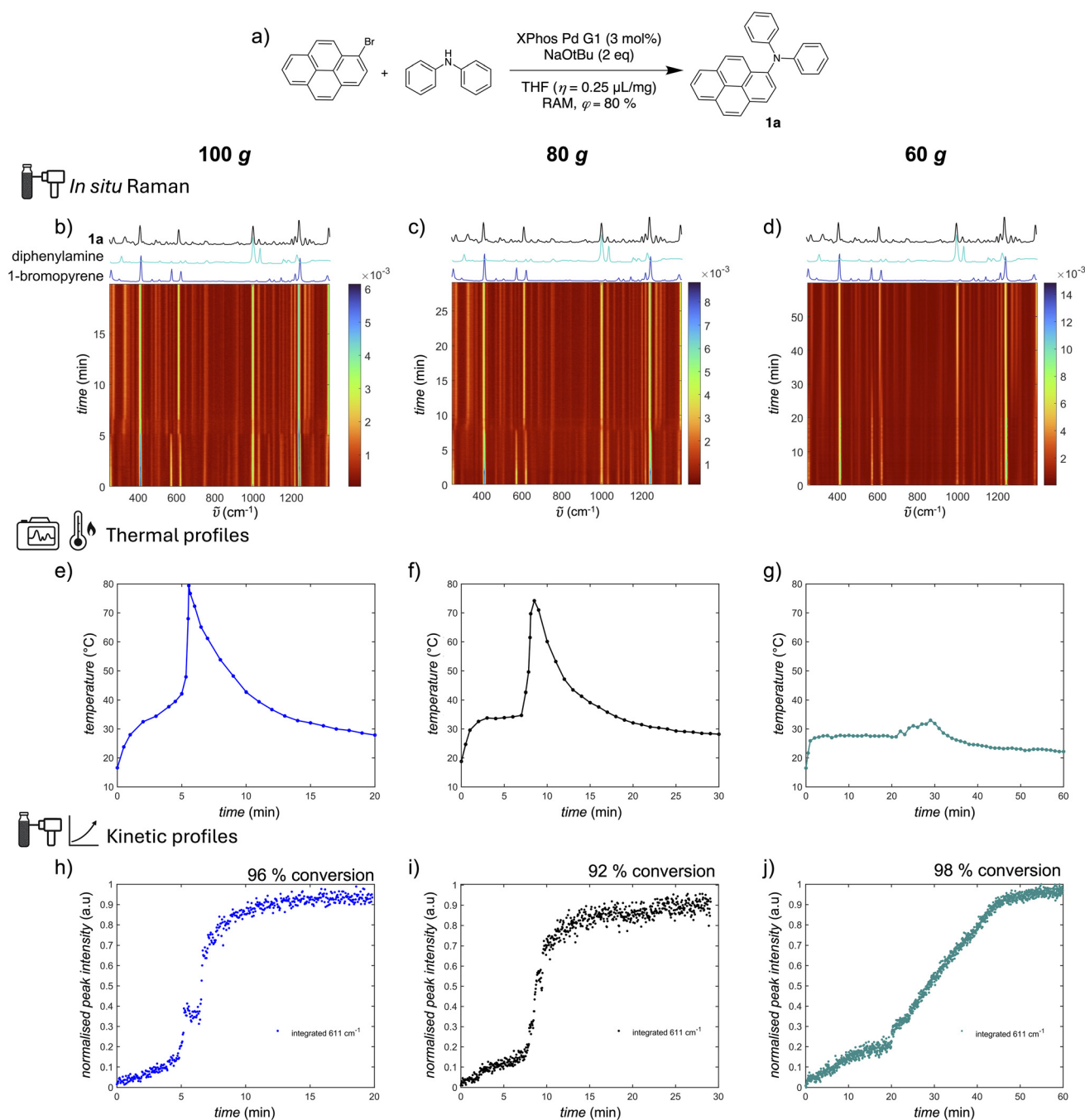


**Fig. 3** Real-time measured thermal profile of the reaction mixture in the presence (3 mol%, red, full conversion) and absence (blue, no reaction) of palladium catalyst (XPhos-Pd-G1). Reaction conditions: diphenylamine (1 equivalent, 4.5 mmol), 1-bromopyrene (1 equivalent, 4.5 mmol), NaOtBu (2 equivalents, 9 mmol), THF ( $\eta = 0.25 \mu\text{L mg}^{-1}$ ), 100g,  $\varphi \approx 80\%$ .





respectively. In contrast, Raman profiles of reactions conducted at 60g showed a more linear reaction profile, with full conversion reached after *ca.* 1 hour (Fig. 4, also see SI Fig. S12). Immediate analysis of the reaction mixture after 60 minutes of RAM showed 98% conversion to **1a**. Overall, the

reaction time required to reach quantitative conversion at 60g is comparable to the previously reported ball-milling work,<sup>33</sup> but working at 80g and 100g led to significant reaction acceleration, shown to be associated with rapid, autogenous heating. The change in kinetic behaviour upon changing the



system acceleration is reminiscent of behaviour previously reported in ball-milling reactions, where decreasing the milling frequency led to a similar change from sigmoidal to apparently more linear-like kinetics.<sup>53</sup>

Real-time THz-Raman monitoring revealed that the formation of crystalline **1a** is preceded by a loss of crystallinity of the reaction mixture. At 100g, the THz-Raman spectrum of the reaction mixture lost the sharp features characteristic of crystalline 1-bromopyrene and diphenylamine within *ca.* 5 minutes (Fig. 5a and b), leaving only a single broad signal in the range from the Rayleigh line to *ca.* 75 cm<sup>-1</sup>. A broad signal in THz-Raman spectroscopy is generally consistent with a non-crystalline environment.<sup>54,55</sup> Moreover, a similar THz-Raman signal is also observed upon melting a freshly prepared reaction mixture on a thermally controlled sample stage, without a liquid additive, indicating that the reaction environment in RAM prior to formation of crystalline **1a** resembles a melt (see SI Fig. S16 and S17). While liquid intermediate phases, such as eutectics, have been noted in solventless and mechanochemical reactions,<sup>51,52</sup> their behaviour has generally been described only in qualitative terms. In this case, however, non-negative least-squares (NNLS) fitting<sup>47,53</sup> (see SI Section S1.8) of the THz-Raman spectra of each reaction component, including that of the non-crystalline intermediate, provides an opportunity to analyze the appearance of such phases in a more detailed fashion. The representative spectrum of the non-crystalline intermediate was selected from the real-time measurement (experimental frame 121, see Fig. 5c) and NNLS analysis indicated that the intermediate becomes increasingly prominent over *ca.* 5 minutes and then rapidly decays, concomitant with the appearance of THz-Raman bands characteristic of crystalline **1a**. Based on a non-quantitative relative spectral contribution analysis, the relative amount of crystalline **1a** appears to develop following a sigmoid curve, simultaneously with the formation of Raman bands characteristic of **1a** in the fingerprint-Raman region. Overall, these observations indicate that the reaction at 100g is mediated by a non-crystalline, melt-like phase from which the crystalline **1a** appears. This observation might also be of potential relevance to analogous ball-milling reaction designs. Comparing the real-time spectroscopic and thermal monitoring data for reactions conducted at 80g or 100g indicates that the temperature spike is closely associated with a rapid, sigmoidal increase in product formation. This temperature increase is almost completely absent when conducting the reaction at a lower acceleration of 60g, with the reaction profile now appearing approximately linear. This observation suggests that one approach to control thermal and kinetic behaviour of reactions conducted by RAM is by varying acceleration. Alternatively, we also find that temperature increase in RAM can also be avoided by reducing  $\varphi$ . This is illustrated by conducting the reaction using the same amount of starting material (4.5 mmol), but in a glass vial of approximately double the volume (5 mL *vs.* 9 mL, see SI Fig. S1) and similar internal diameter (13.2 mm *vs.* 14.7 mm, respectively), effectively reducing  $\varphi$  to *ca.* 40%. The reaction exhibited a significantly smaller temperature increase, to *ca.*

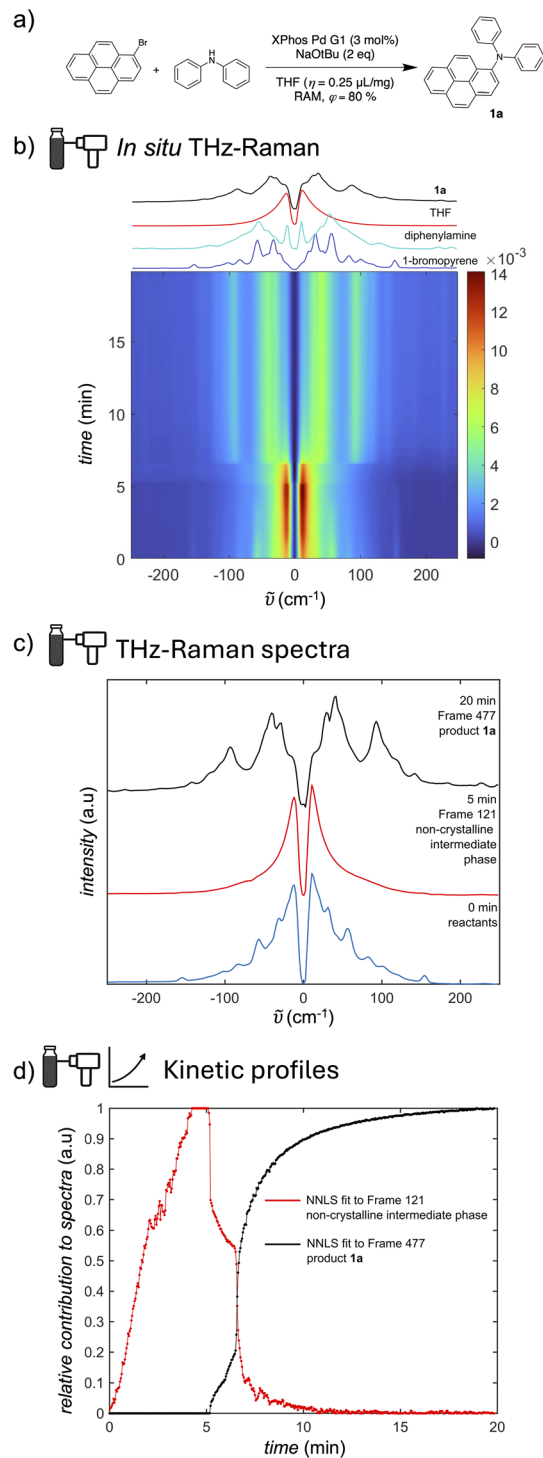


**Fig. 5** Real-time THz-Raman monitoring of the RAM Buchwald–Hartwig amination of 1-bromopyrene and diphenylamine to form **1a** at 100g: (a) reaction scheme; (b) time-resolved THz-Raman spectrum of the reaction; (c) selected individual spectra (frames) collected after 0, 5 and 20 minutes of RAM, representing the spectra of the reactants, the non-crystalline intermediate and the product, that were used for NNLS fitting. (d) Change in spectral contribution of the non-crystalline intermediate (red) and crystalline product **1a** (black), as established by NNLS fitting of THz-Raman spectra for the intermediate (representative spectrum is frame 121, collected at *~* 5 min, shown in panel 4b, red), and **1a** (representative spectrum is frame 477, collected at *~* 20 min, shown in panel 4b, black).



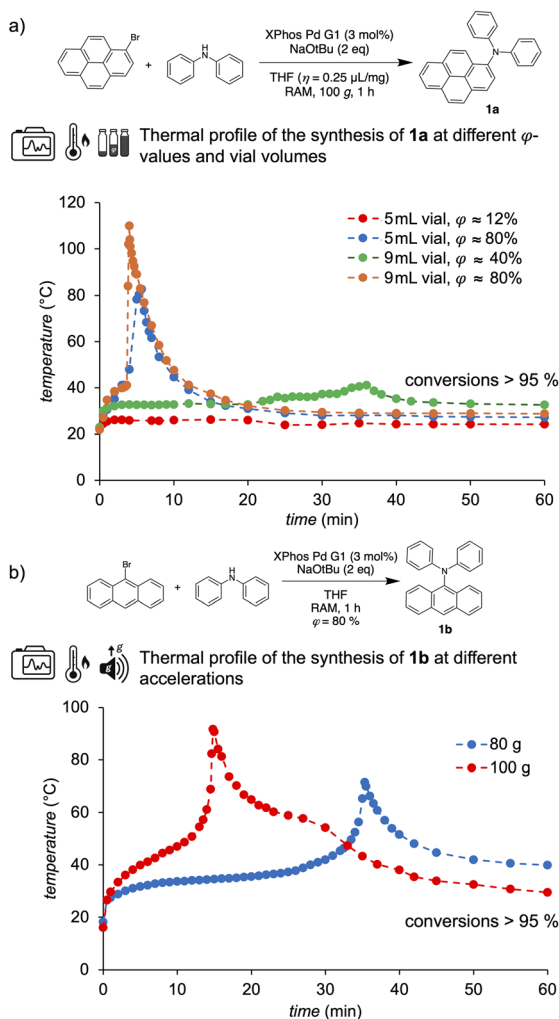


**Fig. 6** Thermal monitoring data for the Buchwald–Hartwig coupling of diphenylamine with (a) 1-bromopyrene to form **1a** at 100g at different  $\varphi$ -values (12, 40 and 80%) and vial volumes (5 and 9 mL) and (b) 9-bromoanthracene to form **1b** at accelerations of 80g and 100g (for  $\varphi \approx 80\%$ ). All  $\varphi$  values are approximate and correspond to the filling level of the initial reaction mixture, before the onset of RAM.

35 °C (Fig. 6a), while reaction conversion after 60 minutes of RAM was found by  $^1\text{H}$  NMR to be >95%.

Conversely, if both the volume of the reaction vial and the scale of the reaction are doubled, *i.e.*, maintaining the same initial  $\varphi$ -value (*ca.* 80%), a short-lived temperature increase is again observed (90 to 110 °C) within 4 minutes (Fig. 6a). It is not yet clear why changing  $\varphi$ , but using the same amount of material, influences reaction progress. Potential explanations might include general differences in mixing, differences in heat dissipation due to sample being more scattered across the reactor at low  $\varphi$ , or the reactor lid acting as a secondary transducer of mechanical energy to the reaction mixture at higher  $\varphi$ . We note that mixing under RAM conditions is an area of active study.<sup>29,30</sup>

A similar thermal profile at high acceleration was also observed for the coupling of 9-bromoanthracene and diphenyl-

amine to form **1b**. At 100g and 80g (both at  $\varphi = 80\%$ ) a temperature spike appeared, similar to what was observed for the synthesis of **1a**. However, this was only observed after approximately 15 minutes and 35 minutes of mixing at 100g and 80g, respectively (Fig. 6b, also SI Fig. S18). Simultaneous real-time *in situ* monitoring of the synthesis of **1a** with THz-Raman spectroscopy suggests that the appearance of a thermal spike is not related to RAM-induced friction, but instead correlates with the reaction event. In such a scenario, the observed thermal signature would indicate that the coupling of diphenylamine with 9-bromoanthracene is already highly advanced after 15 minutes at 100g. Indeed, analysis of the reaction mixture after 15 minutes by  $^1\text{H}$  NMR spectroscopy revealed 74% conversion to **1b**. Overall, the real-time measured thermal profiles reveal a significant temperature evolution in the Buchwald–Hartwig amination by RAM, related not to frictional heating but to the chemical transformation. This, together with the appearance of an induction period followed by a clear temperature spike, as opposed to a continuous increase in temperature, represents a behaviour similar to mechanically-induced self-propagating reactions (MSRs), typically observed in highly exothermic inorganic mechanochemical reactions.<sup>56</sup>

Having observed that higher  $\varphi$  and acceleration values lead to improved conversions to **1a** and **1b**, we explored whether such behaviour will be seen for a wider range of reactants (Table 1). A broader set of reactions were explored in triplicate both under the highly effective conditions of 100g,  $\varphi \approx 80\%$ , and under the initially explored conditions of 60g,  $\varphi \approx 12\%$ , that would be somewhat similar to those found in a ball-milling design. Moreover, we have also explored how the reaction conversion at 60g,  $\varphi \approx 12\%$  changes with  $\eta$ , allowing us to determine the  $\eta$ -value at which the conversion reaches a maximum ( $\eta_{\text{max}}$ ).<sup>4,6</sup> This enabled also the comparison of reactivity at 60g,  $\varphi \approx 12\%$  under  $\eta$ -optimized conditions, to reactivity at 100g,  $\varphi \approx 80\%$  and a set, non-optimized small  $\eta$ -value. The results (Table 1), in almost all cases, show 80% to 90% conversions within 10 minutes of RAM at 100g and  $\varphi \approx 80\%$ . Importantly, these conditions permitted high-yielding reactions to be readily achieved without extensive  $\eta$ -screening, with the amount of liquid additive simply set in the range 0.25–0.50  $\mu\text{L mg}^{-1}$ . For **1b**, a longer time of 60 minutes was needed to obtain high reactant conversions (>95%), while for **1f** and the aliphatic amine morpholine (**1t**), the conversion remained in the 40% range. In contrast, reactions conducted at 60g,  $\varphi \approx 12\%$ , either at the same  $\eta$ -value or at  $\eta_{\text{max}}$ , resulted in generally worse conversions even after one hour. For example, conversion to **1a** ( $\eta = 0.25 \mu\text{L mg}^{-1}$ ) was only  $30\% \pm 2$  after 1 hour (Fig. 6a and Table 1).

With a clearer understanding of RAM reaction parameters, we next explored increasing the reaction scale to 100 mmol (total weight 66.5 g) for the synthesis of **1a** (Fig. 7). This 22-fold increase in reaction scale (from initially 4.5 mmol, total weight 3.0 g) was performed by adjusting the quantity of all materials accordingly and using a 100 mL vessel (see SI Fig. S1 and S7). Considering the potential of exothermic behav-



**Table 1** Comparison of the effectiveness of the Buchwald–Hartwig amination under different liquid-assisted RAM conditions, comparing conversion achieved after 10 minutes at 100g,  $\varphi \approx 80\%$  to conversion achieved after 1 hour at 60g,  $\varphi \approx 12\%$ . Conversions are based on triplicate experiments, through  $^1\text{H}$  NMR analysis of crude reaction mixtures immediately after the RAM experiment

Method comparison for different $\varphi$ -values, accelerations, $\eta$ -values and reaction times					
Conditions for $\varphi \approx 12\%$ : 60 g, 1 hour Conditions for $\varphi \approx 80\%$ : 100 g, 10 minutes or a) 1 hour					
$\varphi \approx 12\%$	53% $\pm$ 4 ( $\eta_{\text{max}} = 1.50 \mu\text{L}/\text{mg}$ ) 30% $\pm$ 2 ( $\eta = 0.25 \mu\text{L}/\text{mg}$ )	21% $\pm$ 3 ( $\eta_{\text{max}} = 1.50 \mu\text{L}/\text{mg}$ ) 17% $\pm$ 2 ( $\eta = 0.50 \mu\text{L}/\text{mg}$ )	13% $\pm$ 1 ( $\eta_{\text{max}} = 0.25 \mu\text{L}/\text{mg}$ )	99% $\pm$ 0 ( $\eta_{\text{max}} = 0.25 \mu\text{L}/\text{mg}$ ) 96% $\pm$ 1 ( $\eta = 0.00 \mu\text{L}/\text{mg}$ )	13% $\pm$ 2 ( $\eta_{\text{max}} = 0.25 \mu\text{L}/\text{mg}$ )
$\varphi \approx 80\%$	96% $\pm$ 1 ( $\eta = 0.25 \mu\text{L}/\text{mg}$ )	98% $\pm$ 1 ( $\eta = 0.50 \mu\text{L}/\text{mg}$ ) <sup>a</sup>	87% $\pm$ 2 ( $\eta = 0.25 \mu\text{L}/\text{mg}$ )	92% $\pm$ 1 ( $\eta = 0.00 \mu\text{L}/\text{mg}$ )	96% $\pm$ 1 ( $\eta = 0.25 \mu\text{L}/\text{mg}$ )
$\varphi \approx 12\%$	7% $\pm$ 1 ( $\eta_{\text{max}} = 0.37 \mu\text{L}/\text{mg}$ ) 4% $\pm$ 1 ( $\eta = 0.25 \mu\text{L}/\text{mg}$ )	70% $\pm$ 3 ( $\eta_{\text{max}} = 0.50 \mu\text{L}/\text{mg}$ ) 58% $\pm$ 4 ( $\eta = 0.25 \mu\text{L}/\text{mg}$ )	70% $\pm$ 2 ( $\eta_{\text{max}} = 0.50 \mu\text{L}/\text{mg}$ ) 54% $\pm$ 3 ( $\eta = 0.25 \mu\text{L}/\text{mg}$ )	99% $\pm$ 0 ( $\eta_{\text{max}} = 0.75 \mu\text{L}/\text{mg}$ ) 92% $\pm$ 1 ( $\eta = 0.00 \mu\text{L}/\text{mg}$ )	99% $\pm$ 0 ( $\eta_{\text{max}} = 0.00 \mu\text{L}/\text{mg}$ )
$\varphi \approx 80\%$	48% $\pm$ 3 ( $\eta = 0.25 \mu\text{L}/\text{mg}$ ) <sup>a</sup>	87% $\pm$ 3 ( $\eta = 0.25 \mu\text{L}/\text{mg}$ )	93% $\pm$ 1 ( $\eta = 0.25 \mu\text{L}/\text{mg}$ )	87% $\pm$ 1 ( $\eta = 0.00 \mu\text{L}/\text{mg}$ )	94% $\pm$ 2 ( $\eta = 0.00 \mu\text{L}/\text{mg}$ )
$\varphi \approx 12\%$	99% $\pm$ 0 ( $\eta_{\text{max}} = 1.00 \mu\text{L}/\text{mg}$ ) 55% $\pm$ 3 ( $\eta = 0.00 \mu\text{L}/\text{mg}$ )	99% $\pm$ 0 ( $\eta_{\text{max}} = 0.50 \mu\text{L}/\text{mg}$ ) 60% $\pm$ 4 ( $\eta = 0.00 \mu\text{L}/\text{mg}$ )	96% $\pm$ 2 ( $\eta_{\text{max}} = 0.75 \mu\text{L}/\text{mg}$ ) 83% $\pm$ 3 ( $\eta = 0.25 \mu\text{L}/\text{mg}$ )	99% $\pm$ 0 ( $\eta_{\text{max}} = 0.25 \mu\text{L}/\text{mg}$ )	79% $\pm$ 4 ( $\eta_{\text{max}} = 1.50 \mu\text{L}/\text{mg}$ ) 58% $\pm$ 5 ( $\eta = 0.25 \mu\text{L}/\text{mg}$ )
$\varphi \approx 80\%$	93% $\pm$ 0 ( $\eta = 0.00 \mu\text{L}/\text{mg}$ )	95% $\pm$ 2 ( $\eta = 0.00 \mu\text{L}/\text{mg}$ )	95% $\pm$ 1 ( $\eta = 0.25 \mu\text{L}/\text{mg}$ )	91% $\pm$ 2 ( $\eta = 0.25 \mu\text{L}/\text{mg}$ )	81% $\pm$ 5 ( $\eta = 0.25 \mu\text{L}/\text{mg}$ )
$\varphi \approx 12\%$	88% $\pm$ 3 ( $\eta_{\text{max}} = 0.75 \mu\text{L}/\text{mg}$ ) 60% $\pm$ 5 ( $\eta = 0.00 \mu\text{L}/\text{mg}$ )	98% $\pm$ 1 ( $\eta_{\text{max}} = 0.50 \mu\text{L}/\text{mg}$ ) 94% $\pm$ 2 ( $\eta = 0.25 \mu\text{L}/\text{mg}$ )	97% $\pm$ 1 ( $\eta_{\text{max}} = 0.37 \mu\text{L}/\text{mg}$ ) 88% $\pm$ 3 ( $\eta = 0.25 \mu\text{L}/\text{mg}$ )	99% $\pm$ 0 ( $\eta_{\text{max}} = 0.25 \mu\text{L}/\text{mg}$ )	27% $\pm$ 5 ( $\eta_{\text{max}} = 0.37 \mu\text{L}/\text{mg}$ ) 25% $\pm$ 3 ( $\eta = 0.25 \mu\text{L}/\text{mg}$ )
$\varphi \approx 80\%$	91% $\pm$ 2 ( $\eta = 0.00 \mu\text{L}/\text{mg}$ )	94% $\pm$ 2 ( $\eta = 0.25 \mu\text{L}/\text{mg}$ )	85% $\pm$ 2 ( $\eta = 0.25 \mu\text{L}/\text{mg}$ )	95% $\pm$ 2 ( $\eta = 0.25 \mu\text{L}/\text{mg}$ )	44% $\pm$ 10 ( $\eta = 0.25 \mu\text{L}/\text{mg}$ ) <sup>a</sup>

<sup>a</sup> Reaction conducted for 60 minutes at 100g. All experiments were done in triplicate and NMR analysis was carried out immediately after RAM either by dissolving approximately one-half of the sample in  $\text{DMSO-}d_6$  to which a small amount of water was added to quench the residual strong base  $\text{NaOtBu}$  (**1d**, **1f–1i** and **1n–1t**), or by quenching with water, followed by rapid extraction into  $\text{CDCl}_3$  (**1a–1c**, **1e**, **1m**), depending on product solubility. To ensure that the reaction does not noticeably proceed during NMR analysis, the spectrum for the synthesis of **1a** was measured immediately after RAM ( $\varphi \approx 12\%$ , 1 h, 60g), and then again after *ca.* 1 hour, without any significant change. For all compounds,  $\eta$ -screening was performed in the 0–1.5  $\mu\text{L mg}^{-1}$  range under standard conditions (1 hour, 60g,  $\varphi = 12\%$ ), and the conversions at  $\eta_{\text{max}}$ <sup>4,6</sup> are reported in the Table.

our revealed by smaller-scale *in situ* measurements, the reaction was conducted in a borosilicate jar with a lid capable of withstanding temperatures of up to 140 °C. Real-time monitoring of the reaction at 60g, with  $\varphi$  at *ca.* 70% and  $\eta$ -value of 0.25  $\mu\text{L mg}^{-1}$  revealed the appearance of an exotherm reaching up to 85 °C within 6 minutes, with Raman spectroscopy indicating that the reaction might be essentially complete within *ca.* 15 minutes (Fig. 7b, d and f). Subsequent analysis of the reaction mixture after a total of 60 minutes RAM, by sampling at five different locations in the reaction jar, demonstrated almost complete conversion (98% for all sections), which was also confirmed by a repeat experiment (conversion in the range 94%–95% for six sections of the sample). Overall, increasing the reaction scale led to an increase in reaction kinetics compared to experiments at 4.5 mmol level, which is probably related to less efficient cooling of the larger reaction mixture.

According to real-time Raman spectroscopy data and subsequent NMR analysis (Fig. 7b, d and f), the increased reaction kinetics at a 100 mmol scale enabled the reaction to be completed within 15 minutes using 3 mol% catalyst. This significantly exceeds the size and speed of the previously reported LAG ball-milling approach, and confirms the potential of RAM-based reactions for scale-up without bulk solvents.<sup>3,15</sup> Encouraged by this result, we also explored the reaction at 100 mmol scale using 1 mol% amount of catalyst (Fig. 7c, e and g). Reducing the amount of catalyst still led to almost complete conversion to **1a**, although within *ca.* 80 minutes, as indicated by real-time Raman spectroscopy, and subsequent NMR analysis. Specifically, the reaction at 1 mol% catalyst and 100 mmol scale exhibited an extended period of reaction activation, with an exothermic signal appearing only at *ca.* 40 minutes into the RAM process, concomitant with a sigmoidal increase in reaction progress. We note that the total power



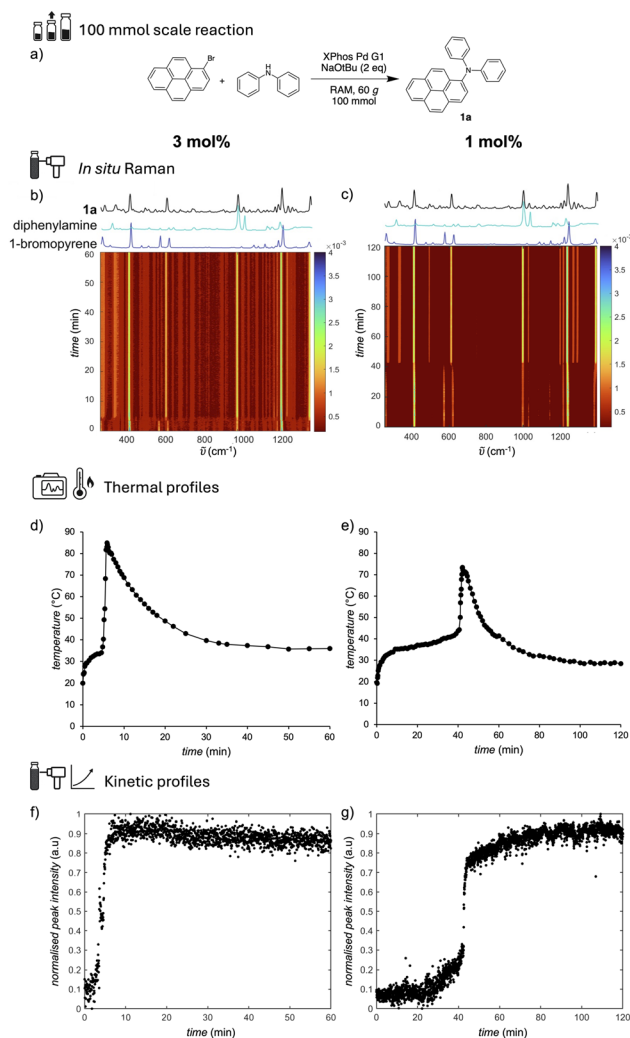


**Fig. 7** Results of real-time thermal and Raman spectroscopy monitoring of the (a) 100 mmol scale RAM Buchwald–Hartwig amination of 1-bromopyrene and diphenylamine to give **1a** using either 3 or 1 mol% of XPhos Pd G1 at acceleration of 60g; (b and c) Raman spectroscopy time-resolved water-fall plot for the reaction run with (b) 3 mol% and (c) 1 mol% of catalyst; (d and e) *in situ* thermography data for reactions run with (d) 3 mol% and (e) 1 mol% of XPhos Pd G1; (f and g) reaction profiles based on peak integration of Raman band at 611  $\text{cm}^{-1}$  for reactions run with (f) 3 mol% and (g) 1 mol%. Reaction conditions: diphenylamine (100 mmol), 1-bromopyrene (100 mmol), NaOtBu (200 mmol), XPhos Pd G1 (3 or 1 mol%), THF ( $\eta = 0.25 \mu\text{L mg}^{-1}$ ),  $\varphi \approx 70\%$ .

consumption of the RAM instrument may vary depending on the acceleration. Power consumption tests conducted using an equivalent weight of sand indicate that operating a 100 mmol reaction at 60g consumes *ca.* 39% less power (103 W) compared to an analogous process at 100g (169 W). In context of reaction design this suggests that longer reaction times at lower accelerations might be partially offset by lower power requirements.

In order to estimate the maximum temperature (maximum adiabatic change in temperature,  $\Delta T_{\text{AD}}$ ) that could be reached during the RAM-based Buchwald–Hartwig coupling reaction,

we conducted a set of DSC experiments to measure the heat released ( $Q$ ) and the heat capacity of the reaction mixture ( $C_p$ ). The ratio of these values is expected to provide  $\Delta T_{\text{AD}}$ ,<sup>57</sup> and similar approaches have previously been used to evaluate the potential of MSRs for self-ignition.<sup>56,58</sup> While the details of the experiments and calculations are provided in the SI (Sections S1.6 and S8), it is important to note that, compared to reactions in homogeneous solution, evaluation of the  $\Delta T_{\text{AD}}$  for a liquid-assisted reaction system is complicated by the exothermic signal of the reaction being affected by endothermic processes, such as the melting of reactants or their dissolution in the small amount of liquid additive, as well as by the  $C_p$  of the reaction mixture changing due to change in composition or state of aggregation. With these limitations in mind, the DSC analyses indicated a  $\Delta T_{\text{AD}}$  value in the range of 90–110 °C. Estimating that frictional heating could increase the initial reaction mixture temperature to *ca.* 50 °C (Fig. 3), such a  $\Delta T_{\text{AD}}$  value indicates that the reaction could reach maximum temperatures in the range of 140–160 °C. Whereas borosilicate vessels used in present real-time monitoring experiments are expected to withstand temperatures to *ca.* 140 °C, and herein monitored small-scale reactions have not been observed to reach temperatures greater than 110 °C, the estimated  $\Delta T_{\text{AD}}$  indicates that further scaling-up is likely to require the use of vessels of greater temperature and pressure robustness, with liquid additives of higher boiling points such as MeOBz being preferred to THF. Most importantly, the estimated  $\Delta T_{\text{AD}}$  is consistent with previous observations of exothermicity in Buchwald–Hartwig aminations,<sup>26</sup> and highlights the importance of the herein explored strategies to control the reaction kinetics and thermal behaviour of the reaction using the RAM setup (for example, by modifying  $\varphi$  and/or acceleration).

Finally, the potential for stoichiometric selectivity in the RAM-based Buchwald–Hartwig aminations was explored through reactions of the primary amine 3,5-dimethoxyaniline with one or two equivalents of an aryl bromide (Fig. 8a). Notably, such an approach to triarylamines was recently explored under ball-milling conditions, requiring external heating.<sup>43</sup> We conducted the reactions using one equivalent of either 3-bromotoluene (a liquid) or 4-bromobenzonitrile (a solid) as the aryl bromide, in the presence of two equivalents of NaOtBu, and methyl benzoate (MeOBz) as the liquid additive ( $\eta = 0.5 \mu\text{L mg}^{-1}$ ), initially at  $\varphi \approx 12\%$  and an acceleration of 60g. After 1 hour of RAM, reactions with one equivalent of the aryl bromide showed complete conversion to the expected diarylamine<sup>59</sup> coupling products **1u** or **1v**. Increasing the acceleration to 100g and  $\varphi$  to *ca.* 95%, greatly accelerated the synthesis, resulting in 98% conversion to **1u** or **1v** after 10 minutes.

Conducting the reactions using two equivalents of the aryl bromide and four equivalents of NaOtBu, however, yielded only **1u** or **1v** at  $\varphi \approx 12\%$ , after 1 hour of RAM at 60g. The targeted 1:2 coupling products could be obtained by modifying  $\varphi$ , acceleration, and the  $\eta$ -value. Specifically, screening the reaction of 3-bromotoluene at different  $\varphi$ -values, while maintaining an acceleration of 100g and  $\eta = 0.25 \mu\text{L mg}^{-1}$ , revealed



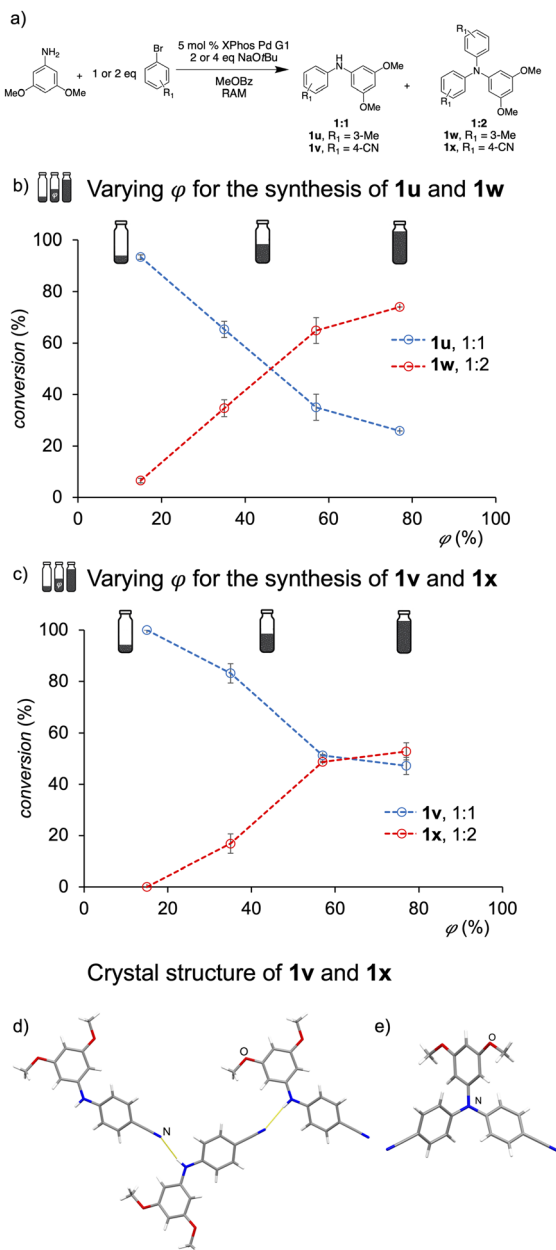


**Fig. 8** Stoichiometric selectivity of the Buchwald–Hartwig amination reaction using RAM: (a) the model coupling reaction and (b) the  $\phi$ -dependent formation of the 1:1 or 2:1 coupling products with 3,5-dimethoxyaniline following RAM at 100g for 2 hours with MeOBz as liquid additive for 3-bromotoluene at  $\eta = 0.25 \mu\text{L mg}^{-1}$ , and (c) for 4-bromobenzonitrile at  $\eta = 0.75 \mu\text{L mg}^{-1}$ . (d) A chain of molecules held by N–H...N hydrogen bonds (yellow dotted lines) in the crystal structure of **1v** and (e) a single molecule of **1x**, as established by single crystal X-ray diffraction structure analysis. Corresponding plots with respect to reaction scale are shown in the SI.

that lower filling ratios result in the diarylamine **1u**, whereas higher  $\phi$  led to an increased amount of the triarylamine **1w** (Fig. 8b). After two hours of RAM, analysis of the reaction conducted at 100g and  $\phi \approx 80\%$  revealed the formation of **1w** and **1u** in an approximate 74:26 ratio, with no residual 3,5-

dimethoxyaniline, assessed by  $^1\text{H}$  NMR spectroscopy. Similar behaviour was observed with 4-bromobenzonitrile (Fig. 8c).

While **1v** was the only product observed after 2 hours of RAM at 100g and  $\phi = 12\%$ , performing the reaction at  $\phi \approx 80\%$  led to the formation of the triarylamine **1x** in a 53:47 ratio with respect to the diarylamine **1v**, with no residual 3,5-dimethoxyaniline, based on  $^1\text{H}$  NMR analysis. Formation of **1v** and **1x** was also confirmed by single crystal X-ray diffraction structure analysis of crystals grown by vapor diffusion of hexanes into a THF solution of the purified products (Fig. 8d and e).

Interestingly, comparing the RAM reactivity of 3,5-dimethoxyaniline and two equivalents of 3-bromotoluene or 4-bromobenzonitrile with a more conventional reaction design, *i.e.*, stirring (600 rpm) in a concentrated MeOBz environment ( $\eta = 5.0 \mu\text{L mg}^{-1}$ ) at room temperature, resulted in quantitative conversion to only the diarylamines **1u** or **1v**, after 10 minutes and 90 minutes, respectively. Increasing the temperature led to the observation of the triarylamines **1w** and **1x**: after 2 hours at 45 °C **1w** and **1x** were observed in 7% and 11% conversions, respectively, while at 80 °C the reaction after 20 minutes progressed to conversions of **1w** and **1x** of 13% and 29%, respectively, and then stalled possibly due to catalyst degradation (see SI Fig. S42).

## Conclusions

This work establishes experimentally accessible parameters for the design and optimization of reactivity under Resonant Acoustic Mixing (RAM) conditions, and advances the understanding of such processes through real-time insight into the temperature evolution, reaction kinetics and bulk phase transformations. Using the Buchwald–Hartwig reaction as a model system, we have combined systematic screening with integrated real-time *in situ* monitoring of temperature, kinetics and bulk phase transformations, to establish how the amount of liquid additive, filling ratio ( $\phi$ ), and acceleration ( $g$ ) govern reaction behaviour in RAM. We report a clear dependence of the reaction conversion on the filling ratio, as well as the ability to modify the reaction kinetics and the associated reaction thermal profile, by varying  $\phi$  and/or the acceleration. The simultaneous use of real-time infrared thermography and *in situ* fingerprint and THz-Raman spectroscopies provides insight into the relationship between reaction profile and temperature evolution, and enables the detection of a non-crystalline, melt-like intermediate phase without requiring synchrotron X-ray diffraction or having to stop and visually inspect the reaction system. Application of NNLS analysis permitted this non-crystalline intermediate to be tracked and related to the formation of the crystalline Buchwald–Hartwig coupling product. Overall, variation of acceleration and  $\phi$  enables tuning of reactivity to enable either near-quantitative conversions rapidly, often within 10–15 minutes, notably faster than previously reported ball-milling approaches.<sup>33</sup> The reactivity is also influenced by the reaction scale, most likely due to the exothermic nature of the herein explored



Buchwald–Hartwig coupling, which enabled a model reaction to be conducted at a 100 mmol scale within *ca.* 15 minutes and at near-quantitative conversion.

The presented benchtop methodology for real-time *in situ* monitoring of RAM processes, that simultaneously provides information on reaction temperature, progress of a covalent bond-formation, and on the appearance and transformations of bulk crystalline or non-crystalline phases, contributes to the emergence of increasingly multi-pronged methods for real-time observation of mechanochemical reactivity.<sup>27,28,60,61</sup> The importance of such real-time studies is evident from the detection of short-lived temperature spikes during Buchwald–Hartwig coupling process at high accelerations, that resemble MSR behaviour observed in inorganic systems.<sup>58,62</sup> The observation of thermal spikes and the herein presented development of strategies to mitigate them by varying the acceleration or the reaction filling ratio, is expected to guide the design of RAM-based reactions, and most likely also other mechanochemical or solventless reaction strategies,<sup>37,38</sup> in such a way to ensure they are not only more efficient, but also safer.<sup>26,63</sup> Indeed, understanding of how reactivity and heat transfer depend on RAM operating parameters is likely to be of particular importance when considering potential scale-up of RAM processes to large batch-based or even continuous designs,<sup>1</sup> as evidenced here by changes in thermal behaviour upon increasing reaction scale from 4.5 mmol to 100 mmol. Finally, the combined use of fingerprint and low-frequency Raman spectroscopy monitoring is anticipated to facilitate the mechanistic understanding of mechanochemical reactions in which the role of eutectic formation is unclear, such as in the previously proposed “hidden eutectic” reaction systems.<sup>52</sup>

## Conflicts of interest

There are no conflicts to declare.

## Data availability

Details of experimental procedures, along with characterization data, as well as NMR and THz-Raman spectra, thermal monitoring plots and X-ray crystallography information, in PDF format. The authors have cited additional references within the supporting information.

Supplementary information (SI) is available. See DOI: <https://doi.org/10.1039/d6gc00784h>.

CCDC 2373258 and 2373259 contain the supplementary crystallographic data for this paper.<sup>64a,b</sup>

## Acknowledgements

We thank the support of Genentech, Inc., University of Birmingham, Leverhulme Trust (TF, THB), and NSERC CGS-D Scholarship (CBL). Prof. Duncan L. Browne, University College London, is acknowledged for valuable discussions. Dr Jason

Stafford, School of Chemical Engineering, University of Birmingham is acknowledged for providing access to the thermal camera, Dr Mike Jenkins, School of Metallurgy & Materials, University of Birmingham, is acknowledged for access to the DSC. We thank Drs Paul Clarke and Tim Mann, PerkinElmer, for help in heat capacity measurements. LG would like to dedicate this work to the loving memory of her mother, Sylvie Gonnet, whose strength and support are a continuous inspiration.

## References

- C. J. Wright, P. J. Wilkinson, S. E. Gaultier, D. Fossey, A. O. Burn and P. P. Gill, *Propellants, Explos., Pyrotech.*, 2022, **47**, e202100146, DOI: [10.1002/prop.202100146](https://doi.org/10.1002/prop.202100146).
- D. J. am Ende, S. R. Anderson and J. S. Salan, *Process Res. Dev.*, 2014, **18**, 331–341, DOI: [10.1021/op4003399](https://doi.org/10.1021/op4003399).
- L. Gonnet, C. B. Lennox, J.-L. Do, I. Malvestiti, S. G. Koenig, K. Nagapudi and T. Friščić, *Angew. Chem., Int. Ed.*, 2022, **61**, e202115030, DOI: [10.1002/anie.202115030](https://doi.org/10.1002/anie.202115030).
- M. Wohlgemuth, S. Schmidt, M. Mayer, W. Pickhardt, S. Grätz and L. Borchardt, *Chem. – Eur. J.*, 2023, **29**, e202301714, DOI: [10.1002/chem.202301714](https://doi.org/10.1002/chem.202301714).
- F. Effaty, L. Gonnet, S. G. Koenig, K. Nagapudi, X. Ottenwaelder and T. Friščić, *Chem. Commun.*, 2023, **59**, 1010–1013, DOI: [10.1039/D2CC06013B](https://doi.org/10.1039/D2CC06013B).
- (a) L. Gonnet, C. B. Lennox, T. H. Borchers, J. Vainauskas, Y. Teoh, H. M. Titi, C. J. Barrett, S. G. Koenig, K. Nagapudi and T. Friščić, *Faraday Discuss.*, 2023, **241**, 128–149, DOI: [10.1039/D2FD00131D](https://doi.org/10.1039/D2FD00131D); (b) C. Spula, P. M. Preuß, L. Borchardt and S. Grätz, *Chem. – Eur. J.*, 2025, **31**, e202501137, DOI: [10.1002/chem.202501137](https://doi.org/10.1002/chem.202501137); (c) J. D. Thorpe, J. Marlyn, S. G. Koenig and M. J. Damha, *RSC Mechanochem.*, 2024, **1**, 244–249, DOI: [10.1039/D4MR00009A](https://doi.org/10.1039/D4MR00009A); (d) C. B. Lennox, T. H. Borchers, L. Gonnet, C. J. Barrett, S. G. Koenig, K. Nagapudi and T. Friščić, *Chem. Sci.*, 2023, **14**, 7475–7481, DOI: [10.1039/D3SC01591B](https://doi.org/10.1039/D3SC01591B).
- H. M. Titi, J.-L. Do, A. J. Howarth, K. Nagapudi and T. Friščić, *Chem. Sci.*, 2020, **11**, 7578–7584, DOI: [10.1039/D0SC00333F](https://doi.org/10.1039/D0SC00333F).
- E. Hamzehpoor, F. Effaty, T. H. Borchers, A. Wahrhaftig-Lewis, X. Ottenwaelder, T. Friščić and D. F. Perepichka, *Angew. Chem., Int. Ed.*, 2024, **63**, e202404539, DOI: [10.1002/anie.202404539](https://doi.org/10.1002/anie.202404539).
- S. Hutsch, A. Leonard, S. Graetz, M. V. Hoefler, T. Gutmann and L. Borchardt, *Angew. Chem., Int. Ed.*, 2024, **63**, e202403649, DOI: [10.1002/anie.202403649](https://doi.org/10.1002/anie.202403649).
- A. Nari, J. S. Ovens and D. L. Bryce, *RSC Mechanochem.*, 2024, **1**, 50–62, DOI: [10.1039/D3MR00028A](https://doi.org/10.1039/D3MR00028A).
- S. Nagapudi and K. Nagapudi, *Phys. Chem. Chem. Phys.*, 2024, **26**, 12545–12551, DOI: [10.1039/D3CP04713J](https://doi.org/10.1039/D3CP04713J).
- D. J. Eyckens, D. J. Hayne, L. C. Henderson, S. C. Howard, T. J. Raeber, R. Simons, A. L. Wilde, D. Yalcin and B. W. Muir, *Appl. Surf. Sci.*, 2024, **646**, 158865, DOI: [10.1016/j.apsusc.2023.158865](https://doi.org/10.1016/j.apsusc.2023.158865).



- 13 K. Nagapudi, E. Y. Umanzor and C. Masui, *Int. J. Pharm.*, 2017, **521**, 337–345, DOI: [10.1016/j.ijpharm.2017.02.027](https://doi.org/10.1016/j.ijpharm.2017.02.027).
- 14 S. R. Anderson, D. J. am Ende, J. S. Salan and P. Samuels, *Propellants, Explos., Pyrotech.*, 2014, **39**, 637–640, DOI: [10.1002/prep.201400092](https://doi.org/10.1002/prep.201400092).
- 15 (a) D. Kong, L. Yi, A. Nanni and M. Rueping, *Nat. Commun.*, 2025, **16**, 3983, DOI: [10.1038/s41467-025-59358-1](https://doi.org/10.1038/s41467-025-59358-1); (b) J. Marlyn, O. Del Carlo, J. D. Thorpe and M. J. Damha, *Green Chem.*, 2025, **27**, 8313–8318, DOI: [10.1039/d5gc01768h](https://doi.org/10.1039/d5gc01768h); (c) A. Nanni, D. Kong, C. Zhu and M. Rueping, *Green Chem.*, 2024, **26**, 8341–8347, DOI: [10.1039/D4GC01790K](https://doi.org/10.1039/D4GC01790K).
- 16 J. G. Osorio, E. Hernández, R. J. Romañach and F. J. Muzzio, *Powder Technol.*, 2016, **297**, 349–356, DOI: [10.1016/j.powtec.2016.04.035](https://doi.org/10.1016/j.powtec.2016.04.035).
- 17 J. G. Osorio, K. Sowrirajan and F. J. Muzzio, *Adv. Powder Technol.*, 2016, **27**, 1141–1148, DOI: [10.1016/j.apt.2016.03.025](https://doi.org/10.1016/j.apt.2016.03.025).
- 18 J. G. Osorio and F. J. Muzzio, *Powder Technol.*, 2015, **278**, 46–56, DOI: [10.1016/j.powtec.2015.02.033](https://doi.org/10.1016/j.powtec.2015.02.033).
- 19 A. J. Claydon, A. N. Patil, S. Gaulter, G. Kister and P. P. Gill, *Chem. Eng. Process.*, 2022, **173**, 108806, DOI: [10.1016/j.cep.2022.108806](https://doi.org/10.1016/j.cep.2022.108806).
- 20 A. A. L. Michalchuk, K. S. Hope, S. R. Kennedy, M. V. Blanco, E. V. Boldyreva and C. R. Pulham, *Chem. Commun.*, 2018, **54**, 4033–4036, DOI: [10.1039/c8cc02187b](https://doi.org/10.1039/c8cc02187b).
- 21 A. A. L. Michalchuk, E. V. Boldyreva, A. M. Belenguer, F. Emmerling and V. V. Boldyrev, *Front. Chem.*, 2021, **9**, 685789, DOI: [10.3389/fchem.2021.685789](https://doi.org/10.3389/fchem.2021.685789).
- 22 O. Galant, G. Cerfeda, A. S. McCalmont, S. L. James, A. Porcheddu, F. Delogu, D. E. Crawford, E. Colacino and S. Spatari, *ACS Sustainable Chem. Eng.*, 2022, **10**, 1430–1439, DOI: [10.1021/acssuschemeng.1c06434](https://doi.org/10.1021/acssuschemeng.1c06434).
- 23 M. Lavayssiere and F. Lamaty, *Chem. Commun.*, 2023, **59**, 3439–3442, DOI: [10.1039/D2CC06934B](https://doi.org/10.1039/D2CC06934B).
- 24 P. Ruiz-Castillo and S. L. Buchwald, *Chem. Rev.*, 2016, **116**, 12564–12649, DOI: [10.1021/acs.chemrev.6b00512](https://doi.org/10.1021/acs.chemrev.6b00512).
- 25 J. Magano and J. R. Dunetz, *Chem. Rev.*, 2011, **111**, 2177–2250, DOI: [10.1021/cr100346g](https://doi.org/10.1021/cr100346g).
- 26 (a) Q. Yang, N. R. Babij and S. Good, *Org. Process Res. Dev.*, 2019, **23**, 2608–2626, DOI: [10.1021/acs.oprd.9b00377](https://doi.org/10.1021/acs.oprd.9b00377); (b) N. Marion, O. Navarro, J. Mei, E. D. Stevens, N. M. Scott and S. P. Nolan, *J. Am. Chem. Soc.*, 2006, **128**, 4101–4111, DOI: [10.1021/ja057704z](https://doi.org/10.1021/ja057704z); (c) O. Navarro, N. Marion, J. Mei and S. P. Nolan, *Chem. – Eur. J.*, 2006, **12**, 5142–5148, DOI: [10.1002/chem.200600283](https://doi.org/10.1002/chem.200600283); (d) O. P. Schmidt and D. G. Blackmond, *ACS Catal.*, 2020, **10**, 8926–8932, DOI: [10.1021/acscatal.0c01929](https://doi.org/10.1021/acscatal.0c01929).
- 27 (a) H. Kulla, M. Wilke, F. Fischer, M. Röllig, C. Maierhofer and F. Emmerling, *Chem. Commun.*, 2017, **53**, 1664–1667, DOI: [10.1039/c6cc08950j](https://doi.org/10.1039/c6cc08950j); (b) S. Krause Hinojosa, T. Dogan, S. Fabig, S. Grätz and L. Borchardt, *Chem. – Eur. J.*, 2025, **31**, e01336, DOI: [10.1002/chem.202501336](https://doi.org/10.1002/chem.202501336).
- 28 (a) H. Kulla, S. Haferkamp, I. Akhmetova, M. Röllig, C. Maierhofer, K. Rademann and F. Emmerling, *Angew. Chem., Int. Ed.*, 2018, **57**, 5930–5933, DOI: [10.1002/anie.201800147](https://doi.org/10.1002/anie.201800147); (b) K. Užarević, N. Ferdelji, T. Mrla, P. A. Julien, B. Halasz, T. Friščić and I. Halasz, *Chem. Sci.*, 2018, **9**, 2525–2532, DOI: [10.1039/c7sc05312f](https://doi.org/10.1039/c7sc05312f).
- 29 (a) H. Sezer, D. Werner, J. A. Sykes, N. Bazin, P. Bolton and C. R. K. Windows-Yule, *Chem. Eng. Sci.*, 2025, **306**, 121166, DOI: [10.1016/j.ces.2024.121166](https://doi.org/10.1016/j.ces.2024.121166); (b) S. Zhang, X. Wang and L. Zhang, *Powder Technol.*, 2025, **456**, 120841, DOI: [10.1016/j.powtec.2025.120841](https://doi.org/10.1016/j.powtec.2025.120841).
- 30 L. Vugrin, C. Chatzigiannis, E. Colacino and I. Halasz, *RSC Mechanochem.*, 2025, **2**, 482–487, DOI: [10.1039/D5MR00016E](https://doi.org/10.1039/D5MR00016E).
- 31 Q.-L. Shao, Z.-J. Jiang and W.-K. Su, *Tetrahedron Lett.*, 2018, **59**, 2277–2280, DOI: [10.1016/j.tetlet.2018.04.078](https://doi.org/10.1016/j.tetlet.2018.04.078).
- 32 Q. Cao, W. I. Nicholson, A. C. Jones and D. L. Browne, *Org. Biomol. Chem.*, 2019, **17**, 1722–1726, DOI: [10.1039/C8OB01781F](https://doi.org/10.1039/C8OB01781F).
- 33 K. Kubota, T. Seo, K. Koide, Y. Hasegawa and H. Ito, *Nat. Commun.*, 2019, **10**, 111, DOI: [10.1038/s41467-018-08017-9](https://doi.org/10.1038/s41467-018-08017-9).
- 34 Q. Lemesre, T. Wiesner, R. Wiechert, E. Rodrigo, S. Triebel and H. Geneste, *Green Chem.*, 2022, **24**, 5502–5507, DOI: [10.1039/D2GC01460B](https://doi.org/10.1039/D2GC01460B).
- 35 L. A. Panther, D. P. Guest, A. McGown, H. Emerit, R. K. Tareque, A. Jose, C. M. Dadswell, S. J. Coles, G. J. Tizzard, R. González-Méndez, C. A. I. Goodall, M. C. Bagley, J. Spencer and B. W. Greenland, *Chem. – Eur. J.*, 2022, **28**, e202201444, DOI: [10.1002/chem.202201444](https://doi.org/10.1002/chem.202201444).
- 36 M. M. Heravi, Z. Kheilkordi, V. Zadsirjan, M. Heydari and M. Malmir, *J. Organomet. Chem.*, 2018, **861**, 17–104, DOI: [10.1016/j.jorganchem.2018.02.023](https://doi.org/10.1016/j.jorganchem.2018.02.023).
- 37 M. A. Topchiy, P. B. Dzhevakov, M. S. Rubina, O. S. Morozov, A. F. Asachenko and M. S. Nechaev, *Eur. J. Org. Chem.*, 2016, **2016**, 1908–1914, DOI: [10.1002/ejoc.201501616](https://doi.org/10.1002/ejoc.201501616).
- 38 J.-S. Ouyang, X. Zhang, B. Pan, H. Zou, A. S. C. Chan and L. Qiu, *Org. Lett.*, 2023, **25**, 7491–7496, DOI: [10.1021/acs.orglett.3c02651](https://doi.org/10.1021/acs.orglett.3c02651).
- 39 P. A. Forero-Cortés and A. M. Haydl, *Org. Process Res. Dev.*, 2019, **23**, 1478–1483, DOI: [10.1021/acs.oprd.9b00161](https://doi.org/10.1021/acs.oprd.9b00161).
- 40 K. Kubota, T. Endo, M. Uesugi, Y. Hayashi and H. Ito, *ChemSusChem*, 2022, **15**, e202102132, DOI: [10.1002/cssc.202102132](https://doi.org/10.1002/cssc.202102132).
- 41 For reviews and selected examples on liquid-assisted grinding, see: (a) L. E. Wenger and T. P. Hanusa, *Chem. Commun.*, 2023, **59**, 14210–14222, DOI: [10.1039/D3CC04929A](https://doi.org/10.1039/D3CC04929A); (b) P. Ying, J. Yu and W. Su, *Adv. Synth. Catal.*, 2021, **363**, 1246–1271, DOI: [10.1002/adsc.202001245](https://doi.org/10.1002/adsc.202001245); (c) M. Banerjee, A. A. Bhosle, A. Chatterjee and S. Saha, *J. Org. Chem.*, 2021, **86**, 13911–13923, DOI: [10.1021/acs.joc.1c01540](https://doi.org/10.1021/acs.joc.1c01540); (d) N. K. Narayanan and M. Schnürch, *ChemCatChem*, 2025, **17**, e202401613, DOI: [10.1002/cctc.202401613](https://doi.org/10.1002/cctc.202401613); (e) R. S. Atapalkar and A. A. Kulkarni, *React. Chem. Eng.*, 2024, **9**, 10–25, DOI: [10.1039/D2RE00521B](https://doi.org/10.1039/D2RE00521B); (f) L. Chen, M. Regan and J. Mack, *ACS Catal.*, 2016, **6**, 868–872, DOI: [10.1021/acscatal.5b02001](https://doi.org/10.1021/acscatal.5b02001); (g) M. Arhangelskis, D.-K. Bučar, S. Bordignon, M. R. Chierotti, S. A. Stratford, D. Voinovich, W. Jones and D. Hasa, *Chem. Sci.*, 2021, **12**, 3264–3269, DOI: [10.1039/D0SC05071G](https://doi.org/10.1039/D0SC05071G); (h) J. Breinsperger, N. Podlesnik, F. Mele and M. Schnürch, *Chem. – Eur. J.*,



- 2026, **32**, e03536, DOI: [10.1002/chem.202503536](https://doi.org/10.1002/chem.202503536);
- (i) I. D'Abbrunzo and D. Hasa, *CrystEngComm*, 2026, **28**, 1752–1769, DOI: [10.1039/d5ce00778j](https://doi.org/10.1039/d5ce00778j);
- (j) H. Luo, Z. Huang, Y. Lai, Y. Jiang, T. Wang and K. Yan, *RSC Mechanochem.*, 2026, **3**, 195–200, DOI: [10.1039/d5mr00104h](https://doi.org/10.1039/d5mr00104h);
- (k) P. Freisa, L. Lattuada, A. Barge and G. Cravotto, *RSC Mechanochem.*, 2026, **3**, 144–160, DOI: [10.1039/d5mr00097a](https://doi.org/10.1039/d5mr00097a);
- (l) J. Templ and L. Borchardt, *Angew. Chem., Int. Ed.*, 2026, **65**, e23191, DOI: [10.1002/anie.202523191](https://doi.org/10.1002/anie.202523191);
- (m) J. Yu, H. Chen, Z. Zhang, Y. Fang, T. Ying and W. Su, *Green Chem.*, 2024, **26**, 6570–6577, DOI: [10.1039/D4GC00947A](https://doi.org/10.1039/D4GC00947A);
- (n) P. Ying, T. Ying, H. Chen, K. Xiang, W. Su, H. Xie and J. Yu, *Org. Chem. Front.*, 2024, **11**, 127–134, DOI: [10.1039/D3QO01467C](https://doi.org/10.1039/D3QO01467C).
- 42 T. Friščić, S. L. Childs, S. A. A. Rizvi and W. Jones, *CrystEngComm*, 2009, **11**, 418–426, DOI: [10.1039/B815174A](https://doi.org/10.1039/B815174A).
- 43 K. Kubota, M. Takahashi, F. Puccetti and H. Ito, *Org. Lett.*, 2025, **27**, 5691–5696, DOI: [10.1021/acs.orglett.5c01456](https://doi.org/10.1021/acs.orglett.5c01456).
- 44 J. L. Howard, Y. Sagatov, L. Repousseau, C. Schotten and D. L. Browne, *Green Chem.*, 2017, **19**, 2798–2802, DOI: [10.1039/C6GC03139K](https://doi.org/10.1039/C6GC03139K).
- 45 A. Stolle, Technical Implications of Organic Syntheses in Ball Mills, in *Ball Milling Towards Green Synthesis: Applications, Projects, Challenges*, ed. A. Stolle and B. Ranu, Royal Society of Chemistry, Cambridge, 2015, pp. 241–276.
- 46 S. Lukin, K. Užarević and I. Halasz, *Nat. Protoc.*, 2021, **16**, 3492–3521, DOI: [10.1038/s41596-021-00545-x](https://doi.org/10.1038/s41596-021-00545-x).
- 47 T. Borchers, F. Topić, M. Arhangelskis, M. Ferguson, C. B. Lennox, P. A. Julien and T. Friščić, *Chem*, 2025, **11**, 102319, DOI: [10.1016/j.chempr.2024.09.018](https://doi.org/10.1016/j.chempr.2024.09.018).
- 48 K. L. Nguyen, T. Friščić, G. M. Day, L. F. Gladden and W. Jones, *Nat. Mater.*, 2007, **6**, 206–209, DOI: [10.1038/nmat1848](https://doi.org/10.1038/nmat1848).
- 49 H. Watanabe, R. Hiraoka and M. Senna, *Tetrahedron Lett.*, 2006, **47**, 4481–4484, DOI: [10.1016/j.tetlet.2006.04.030](https://doi.org/10.1016/j.tetlet.2006.04.030).
- 50 M. Senna and A. A. L. Michalchuk, *RSC Mechanochem.*, 2025, **2**, 351–369, DOI: [10.1039/D4MR00084F](https://doi.org/10.1039/D4MR00084F).
- 51 G. Rothenberg, A. P. Downie, C. L. Raston and J. L. Scott, *J. Am. Chem. Soc.*, 2001, **123**, 8701–8708, DOI: [10.1021/ja0034388](https://doi.org/10.1021/ja0034388).
- 52 O. Dolotko, J. W. Wiench, K. W. Dennis, V. K. Pecharsky and V. P. Balema, *New J. Chem.*, 2010, **34**, 25–28, DOI: [10.1039/B9NJ00588A](https://doi.org/10.1039/B9NJ00588A).
- 53 P. A. Julien, I. Malvestiti and T. Friščić, *Beilstein J. Org. Chem.*, 2017, **13**, 2160–2168, DOI: [10.3762/bjoc.13.216](https://doi.org/10.3762/bjoc.13.216).
- 54 G. Walker, P. Römann, B. Poller, K. Löbmann, H. Grohgan, J. S. Rooney, G. S. Huff, G. P. S. Smith, T. Rades, K. C. Gordon, C. J. Strachan and S. J. Fraser-Miller, *Mol. Pharm.*, 2017, **14**, 4675–4684, DOI: [10.1021/acs.molpharmaceut.7b00803](https://doi.org/10.1021/acs.molpharmaceut.7b00803).
- 55 T. Achibat, A. Boukenter, E. Duval, G. Lorentz and S. Etienne, *J. Chem. Phys.*, 1991, **95**, 2949–2954, DOI: [10.1063/1.460896](https://doi.org/10.1063/1.460896).
- 56 L. Takacs, *Prog. Mater. Sci.*, 2002, **47**, 355–414, DOI: [10.1016/S0079-6425\(01\)00002-0](https://doi.org/10.1016/S0079-6425(01)00002-0).
- 57 F. Stoessel, in *Thermal Safety of Chemical Processes, Risk Assessment and Process Design*, Wiley-VCH Verlag, Weinheim, Germany, 2nd edn, 2020.
- 58 Possibility of inorganic MSR under intense mixing conditions was recently described, see: M. Baláž, P. Jacko, M. Bereš, K. Kenges, L. Mussapyrova, S. S. Shahgoli, M. Podobová, K. Szmuc, G. Gruzal, J. Tulková, I. O. Tampubulon, Y. Shpotyuk, U. Aydemir and T. Stolar, *ChemRxiv*, 2026, preprint, DOI: [10.26434/chemrxiv-2025-l4n3s-v2](https://doi.org/10.26434/chemrxiv-2025-l4n3s-v2).
- 59 B. P. Fors, D. A. Watson, M. R. Biscoe and S. L. Buchwald, *J. Am. Chem. Soc.*, 2008, **130**, 13552–13554, DOI: [10.1021/ja8055358](https://doi.org/10.1021/ja8055358).
- 60 C. Leroy, S. Mitteleite, G. Félix, N. Fabregue, J. Špačková, P. Gaveau, T.-X. Métro and D. Laurencin, *Chem. Sci.*, 2022, **13**, 6328–6334, DOI: [10.1039/D2SC01496C](https://doi.org/10.1039/D2SC01496C).
- 61 G. Zgrablić, A. Senkić, N. Vidović, K. Užarević, D. Čapeta, I. Brekalo and M. Rakić, *Phys. Chem. Chem. Phys.*, 2025, **27**, 5909–5920, DOI: [10.1039/D4CP04757E](https://doi.org/10.1039/D4CP04757E).
- 62 M. Baláž, R. Džunda, R. Bureš, T. Sopčák and T. Csanádi, *RSC Mechanochem.*, 2024, **1**, 94–105, DOI: [10.1039/D3MR00001J](https://doi.org/10.1039/D3MR00001J).
- 63 I. Priestley, C. Battilocchio, A. V. Iosub, F. Barreteau, G. W. Bluck, K. B. Ling, K. Ingram, M. Ciaccia, J. A. Leitch and D. L. Browne, *Org. Process Res. Dev.*, 2023, **27**, 269–275, DOI: [10.1021/acs.oprd.2c00226](https://doi.org/10.1021/acs.oprd.2c00226).
- 64 (a) CCDC 2373258: Experimental Crystal Structure Determination, 2026, DOI: [10.5517/ccdc.csd.cc2knkqj](https://doi.org/10.5517/ccdc.csd.cc2knkqj);
- (b) CCDC 2373259: Experimental Crystal Structure Determination, 2026, DOI: [10.5517/ccdc.csd.cc2knkrk](https://doi.org/10.5517/ccdc.csd.cc2knkrk).

